

## ORIGINAL RESEARCH

# BRD4 inhibitor JQ1 may affect the prognosis of cervical cancer through super-enhancer-related genes

Yuxi Lin<sup>1,†</sup>, Bifen Huang<sup>2,†</sup>, Fangjie He<sup>3,4,\*</sup>, Jianqing Zheng<sup>1,5,\*</sup>

<sup>1</sup>The Second Clinical Medical College of Fujian Medical University, The Second Affiliated Hospital of Fujian Medical University, 362000 Quanzhou, Fujian, China

<sup>2</sup>Department of Obstetrics and Gynecology, Quanzhou Medical College People's Hospital Affiliated, 362000 Quanzhou, Fujian, China

<sup>3</sup>Department of Obstetrics and Gynecology, The First People's Hospital of Foshan, 528000 Foshan, Guangdong, China

<sup>4</sup>Department of Gynecology, Fujian Maternity and Child Health Hospital, College of Clinical Medicine for Obstetrics & Gynecology and Pediatrics, Fujian Medical University, 350000 Fuzhou, Fujian, China

<sup>5</sup>Department of Radiation Oncology, The Second Affiliated Hospital of Fujian Medical University, 362000 Quanzhou, Fujian, China

**\*Correspondence**

shmilyhbf@fjmu.edu.cn

(Jianqing Zheng);

hfj5362@fsyy.com

(Fangjie He)

† These authors contributed equally.

**Abstract**

To explore the effects of bromine domain protein 4 (*BRD4*) inhibitor JQ1 on the expression profile of super-enhancer-related genes (SE-genes) in cervical cancer (CC) HeLa cells and construct a prognosis model to explore the potential impact of JQ1 on the prognosis of CC. Whole transcriptome sequencing technology was used to detect changes in the gene expression profiles of JQ1-treated and control cells. Differentially expressed SE-genes were identified by matching *via* the dbCoRC database and Cistrome Data Browser (Cistrome DB). The prognosis of differentially expressed SE-genes was analyzed in the Cancer Genome Atlas (TCGA) dataset based on gene expression status. The Cox proportional risk model and least absolute shrinkage and selection operator (LASSO) regression were used to construct the prognostic model. A total of 1161 SE-genes were identified from dbCoRC and Cistrome DB, among which 1004 SE-genes were successfully matched to the expression profiles of JQ1 transcriptome sequencing. Differential expression analysis identified 110 differentially expressed SE-genes, among which 72 were down-regulated and 38 were upregulated. Then, a 9 SE-gene prognostic model was constructed, and Kaplan-Meier (K-M) curves showed that the high-risk group had significantly poorer clinical survival outcomes ( $p < 0.05$ ). Time-dependent receiver operating characteristic (ROC) curves showed that the 1-year, 2-year and 3-year survival estimation of the proposed model was 0.82, 0.86 and 0.87, respectively, demonstrating excellent performance. JQ1 significantly impacts the SE-genes expression profile of HeLa cells, and the proposed model based on 9 differentially expressed SE-genes may effectively predict the survival outcomes of CC patients. As this study was based on exploratory analysis, further prospective studies are needed to verify the effectiveness of the SE-genes-based prognostic model.

**Keywords**

BRD4 inhibitor; Cervical cancer; Super-enhancer related genes; JQ1; HeLa cells; RNA-Seq

## 1. Introduction

Cervical cancer (CC) is one of the most common types of malignant tumors in women worldwide [?] and is ranked first as the highest incidence cancer in women in China [?]. Although surgery or concurrent radiotherapy can cure more than 60–70% of CC patients, the potential for cancer recurrence and distant metastases still poses a significant threat to patient survival [?]. The heterogeneity of this disease results in different survival outcomes in CC patients receiving standard therapy, such as radical surgery or concurrent radiotherapy [?]. Despite achieving long-term survival in more than 70% of patients, the disease remains a major clinical challenge, with approximately 25–30% of patients experiencing tumor recurrence or distant metastasis. In addition, despite chemotherapy and immunotherapy being important treatments for advanced-stage CC, they cannot cure recurrent or metastatic CC [?].

Therefore, there is an urgent need to identify pharmacological agents and individualized novel prognostic and risk-stratified biomarkers to improve the outcomes of these patients [?].

Tumor heterogeneity is often associated with differences in gene expression. Super-enhancers (SEs) are a type of regulatory domain that exhibit unusually strong transcription-assisted activator binding capabilities [? ?]. Compared to typical enhancers (TEs), SEs have a stronger ability to promote transcription, which is more common in tumor cells where SEs act as oncogenes to recruit enhancer-binding proteins to drive gene expression [?]. When SEs exert biological functions *via* target genes, they are termed SE-associated genes (SESGs) or SE-related genes (SE-genes) [?]. Although a growing number of studies have shown that the presence of SE-genes can significantly affect the survival of various types of cancers [? ?], few have investigated their impact on the prognosis of CC patients.

Bromodomain and extra-terminal protein family (BET) is a new class of transcriptional regulatory proteins that can recognize and bind to acetylated lysine residues on histones to recruit transcriptional activators for chromatin acetylation [? ]. Acetylated chromatin can facilitate transcriptional activation and promote tumorigenesis, and blocking this biological process could inhibit tumor growth and promote the apoptosis of cancer cells [? ? ]. Novel BET inhibitors have been reported to exert anti-tumor effects in various tumors by specifically binding to their BET domain in *in vitro* experiments [? ? ? ]. Additionally, previous *in vivo* and *in vitro* studies have shown that SEs inhibitors (JQ1), a specific inhibitor of bromodomain-containing protein 4 (BRD4), can suppress the expression of important target genes by inhibiting the biological function of SEs in cancer [? ? ]. However, it is unclear whether JQ1 has anti-tumor effects and whether JQ1 can influence the expression of SE-genes.

In this study, we explored the mechanism of JQ1 in CC by conducting high-throughput transcriptome sequencing in JQ1-treated HeLa cells to investigate the changes in the expression profile of SE-genes. Further, since the least absolute shrinkage and selection operator (LASSO) penalized Cox regression is most commonly used for factor screening of prognostic models [? ], this methodology was implemented to construct a prognostic model for CC patients based on 1004 SE-related genes. Also, a gene cluster containing 9 SE-genes (*TP53I3*, *ADCY7*, *NQO2*, *CCDC102A*, *ADM*, *SYTL3*, *PSCA*, *NPR1* and *BAIAP2*) was screened, and a risk score model based on these 9 genes was constructed to predict the overall survival (OS) of CC patients. The workflow of the present study is shown in Fig. ??.

## 2. Materials and methods

### 2.1 Cell culture, CCK-8 cell proliferation assay and cDNA library construction and sequencing

Cell Counting Kit-8 (CCK-8) assay was used to assess the cell viability of CC HeLa cells, verify the inhibitory effects of JQ1 and calculate the optimal inhibitory concentration. Details of HeLa cell culture, CCK-8 cell proliferation assay and cDNA library construction and sequencing are shown in **Supplementary material**.

### 2.2 Data source

The microarray data and corresponding clinical information for CC were obtained from the cancer genome atlas database (TCGA, <https://cancergenome.nih.gov/>). A total of 306 cervical cancer tissue samples and 3 paracervical tissue samples were obtained. The basic clinical information, treatment status and prognosis data were retrieved.

### 2.3 Identification and differential expression analysis (DEA) of super-enhancers related genes

A list of SE-genes was identified from the dbCoRC database and Cistrome Data Browser (Cistrome DB) [? ? ]. The

detailed SE and SE-genes associated with CC are listed in **Supplementary Table 1** and **Supplementary Table 2**. The SE-genes dataset was extracted from the JQ1-treated and control expression matrices from our full transcriptome sequencing data, and DEA was performed using the limma package, with the absolute value of Log2 fold change >1 and corrected  $p < 0.05$  as thresholds for screening differentially expressed genes (DEGs). Differentially expressed SE-genes were extracted for heat map plotting, volcano mapping and various visualizations using the R packages “ggplot2” and “ggtree”.

### 2.4 Functional annotation and pathway enrichment analysis (FAPEA) of differentially expressed SE-genes

Gene Ontology (GO) functional enrichment analysis and Kyoto Encyclopedia of Genes and Genomes (KEGG) pathway enrichment were performed to identify DEGs using the R package clusterProfiler. Significant pathways were identified based on a  $p$  value of  $< 0.05$ .

### 2.5 Construction of protein-protein interaction (PPI) network and screening of the core SE-genes

The interaction network of SE-genes targets was built using the STRING database (version 11.0, <http://string-db.org/>), and the interaction network of core targets was constructed using the Cytoscape software (version 3.9.1). In the built PPI network, the size and color of nodes reflected the degree value, while the thickness of edges reflected the comprehensive score. The core targeted gene sets were re-screened using the Cytoscape plug-in MCODE (molecular complex detection). Each module was ranked according to the results of MCODE analysis, which were identified as the core targets and enriched for GO function and KEGG pathways using the R package “clusterProfiler”.

### 2.6 Construction and evaluation of a prognostic model based on differentially expressed SE-genes

Microarray data and corresponding clinical information from the TCGA database were used for prognostic analysis. Differentially expressed SE-genes were grouped into a high- or a low-expressed group according to the median value of gene expression. To identify significant and potential prognostic genes, LASSO penalized Cox regression analysis was performed using the R package “glmnet” to build predictive models. The optimal lambda ( $\lambda$ ) value was identified based on ten-fold cross-validation. The LASSO models were constructed using two best-fit values ( $\lambda_{\min}$  and  $\lambda_{1se}$ ) calculated by minimizing the mean cross-validated error. Then, time-dependent ROC curve analysis was performed to evaluate the performance of the prognostic model.

To obtain an optimal prognostic model, we integrated the expression levels of candidate genes according to the formula  $RiskScore = \beta_i \times X_i$ , where  $X_i$  is a dichotomous variable, with 0 representing a low expression of genes and 1 representing a high expression, and  $\beta_i$  is the regression coefficient for each candidate gene. The risk score for each patient was

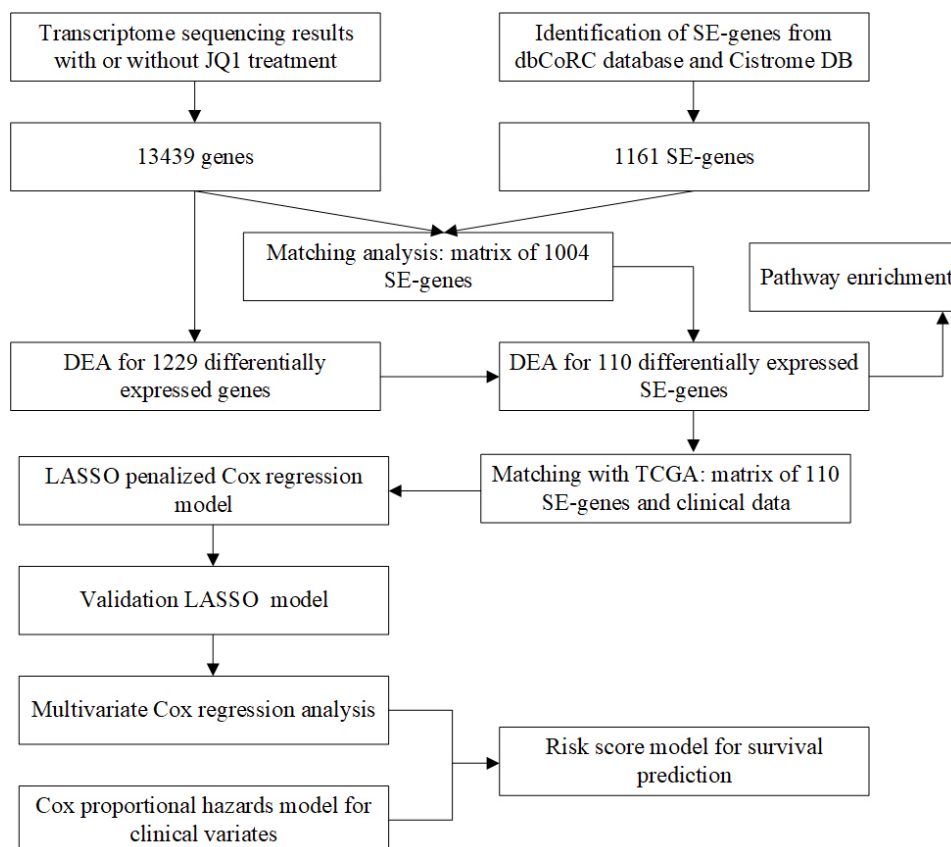


**FIGURE 1. Flow chart of the study design.** SE: super-enhancers; DEA: differential expression analysis; Cistrome DB: Cistrome Data Browser; LASSO: least absolute shrinkage and selection operator; TCGA: The Cancer Genome Atlas.

calculated by weighting the regression coefficients. The best cut-off point was obtained from the maximum standardized long-term statistics, and patients were divided into high-risk and low-risk groups using this best cut-off point.

The prognostic value of the candidate genes was obtained through univariate and multivariate Cox proportional hazard regression models constructed using the R packages “survival” and “survminer”. The calculation results are displayed in the form of forest plots. We further screened other important clinical characteristics to construct a multivariate prognostic model and verify the independence of the constructed prognostic models. The parameters for multivariate prognostic models included the prognostic risk group factor and clinical factors such as age, race, grade, clinical stage, survival with tumor, lymphovascular space invasion, parametrial invasion and uterine involvement. Hazard ratio (HR) with its corresponding 95% confidence interval (CI) and  $p$ -value of each factor were determined. Lastly, the survival ROC package was used to plot the 1-, 2- and 3-year overall survival ROC curves of CC samples.

## 2.7 Statistical analysis

The results of the CCK-8 cell proliferation assay are expressed as mean  $\pm$  standard deviation ( $\bar{x} \pm s$ ) and analyzed using GraphPad Prism version 8.0 (GraphPad Software, San Diego, CA, U.S.A.). One-way ANOVA (Analysis of Variance) or independent samples  $t$ -test was used for data analysis.

Bioinformatics analysis and survival analysis were

performed using the corresponding R packages on the R platform (version 4.2.0). Gene symbols were annotated using the “BiomaRt” package, and DEAs was implemented using the limma package. A two-sided  $p < 0.05$  was considered for determining statistical significance.

## 3. Results

### 3.1 The cell proliferation inhibition rate of JQ1 on HeLa cells *via* CCK-8 assay

The results of the CCK-8 assay showed that the survival rate of HeLa cells decreased with an increase in JQ1 concentration and prolongation of exposure time (Fig. ?? and Table ??). As the semi-inhibitory concentration (IC50) of JQ1 on HeLa cells at 72 h was 1.04  $\mu\text{mol/L}$  under the different concentrations and exposure time, we used 1  $\mu\text{mol/L}$  of JQ1 for 72 h to treat HeLa cells before whole transcriptome resequencing.

### 3.2 Screening and differential expression analysis of SE-genes

A 16 primary HeLa cell-related SEs list was downloaded from the dbCoRC website, and a total of 1161 SE-genes were identified from Cistrome DB *via* the SEs list. The detailed gene list of HeLa cell-related SEs and SE-genes are shown in Fig. ??, **Supplementary Table 1** and **Supplementary Table 2**. Our transcriptome sequencing results revealed a 13,439 gene matrix in HeLa cells with or without JQ1 treatment. A 1004 SE-related gene matrix for HeLa was obtained by overlapping

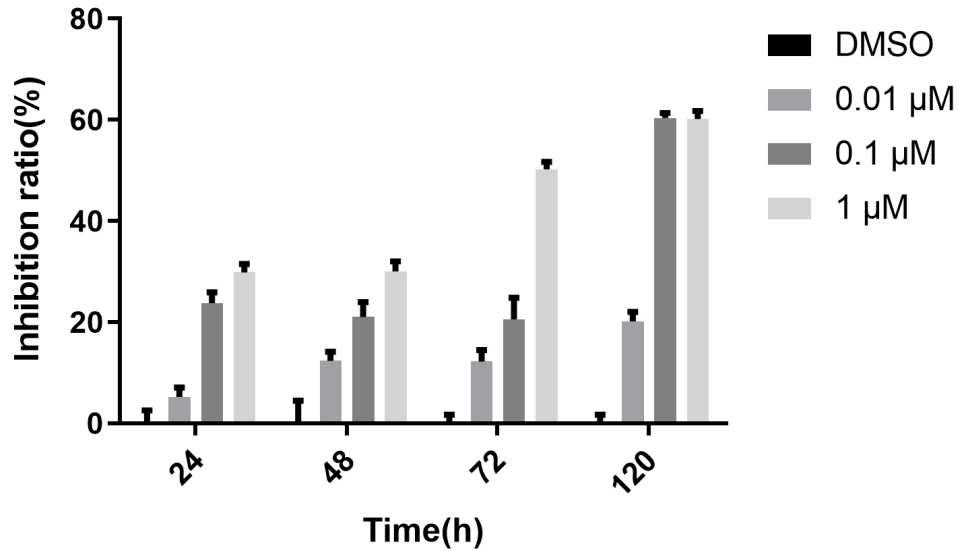


FIGURE 2. The cell proliferation inhibition rate of JQ1 on HeLa cell *via* CCK-8 assay. DMSO: dimethyl sulfoxide.

TABLE 1. The effect of JQ1 on the proliferation of HeLa cells under different concentrations and at different times.

Groups	24 h	48 h	72 h	120 h
DMSO	$-0.02 \pm 2.58$	$0.17 \pm 4.36$	$-0.02 \pm 1.75$	$0.00 \pm 2.58$
0.01 $\mu\text{mol/L}$	$5.23 \pm 1.88$	$12.33 \pm 1.86$	$12.20 \pm 2.30$	$20.17 \pm 1.88$
0.1 $\mu\text{mol/L}$	$23.77 \pm 2.13$	$21.00 \pm 2.97$	$20.58 \pm 4.27$	$60.33 \pm 2.13$
1 $\mu\text{mol/L}$	$29.82 \pm 1.69$	$30.00 \pm 2.00$	$50.22 \pm 1.47$	$60.17 \pm 1.69$
<i>p</i>	<0.001	<0.001	<0.001	<0.001

DMSO: dimethyl sulfoxide.

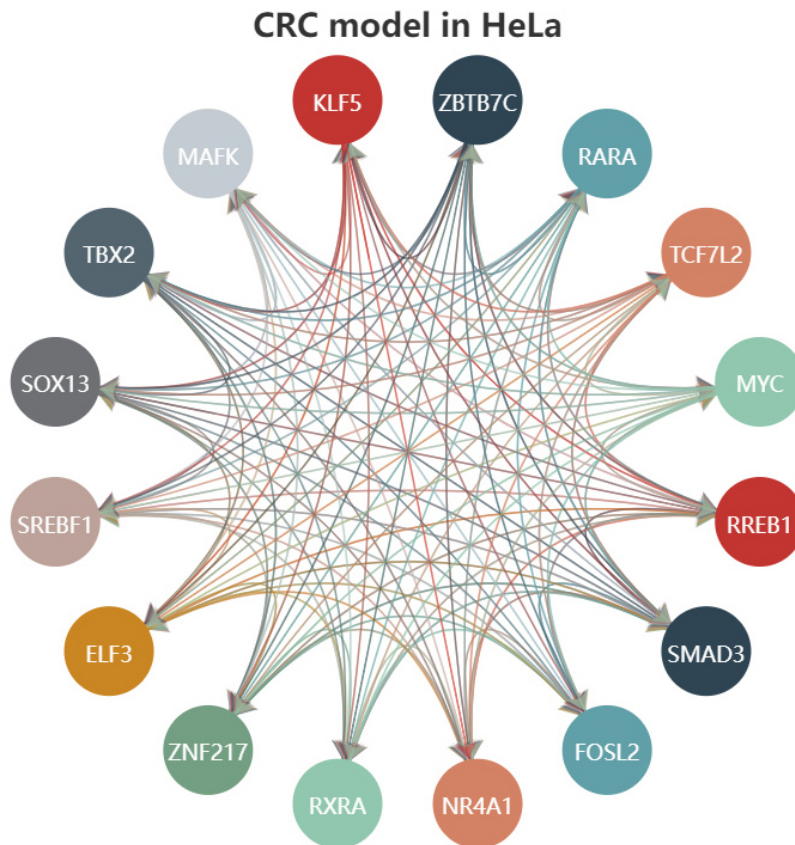


FIGURE 3. Network diagram of HeLa cell-related super-enhancers.

the above two gene sets. Using FDR (false discovery rate)  $<0.05$  and  $\text{LogFC} >1$  as the difference condition, DEA with limma package revealed 110 SE-genes that were differentially expressed, among which 72 genes were downregulated and 38 were upregulated (Fig. ?? and **Supplementary Table 3**).

### 3.3 FAPEA results of differentially expressed SE-genes

The 110 SE-genes were included in FAPEA using the R package clusterProfiler, and the results of the top 15 pathways for each enrichment analysis are shown in Fig. ?? and **Supplementary Table 4**. The top 5 enrichment pathways for DMSO biological processes (BP) were positively associated with the regulation of protein binding, dopaminergic neuron differentiation and regulation of cell shape as well as cyclic nucleotide metabolic process and body morphogenesis. The top 5 enrichment pathways of GO molecular function (MF) were serine-type endopeptidase inhibitor activity, calcium-dependent protein binding, enzyme inhibitor activity, structural constituent of muscle and phospholipase inhibitor activity. The top 5 enrichment pathways of GO cellular component (CC) were collagen-containing extracellular matrix, cell cortex, interstitial matrix, basement membrane, laminin complex. The top 5 enrichment pathways of KEGG were regulation of lipolysis in adipocytes, ECM (extracellular matrix)-receptor interaction, amoebiasis, longevity regulating pathway—multiple species, and focal adhesion.

### 3.4 PPI protein network construction and core module screening of differentially expressed SE-genes

The PPI network of candidate genes was established using the STRING database, and the corresponding node data were imported into the Cytoscape software for subsequent analysis. The PPI map is shown in Fig. ??. The core modules in the PPI network were identified using the MCODE plug-in, and the top 3 modules are shown in Fig. ??. The core module 1 contained 3 genes, namely *LAMC2*, *LAMB3* and *DAG1*. The core module 2 contained 3 genes, namely *TIAMI*, *BAIAP2* and *RHOD*. The core module 3 contained 3 genes, namely *ADCY7*, *GNAL* and *PDE4A*.

### 3.5 Development of the prognostic signature for SE-genes

All of the 110 differentially expressed SE-genes were successfully matched with the TCGA database. The constructed prognostic expression matrix is displayed in **Supplementary Table 5**. Then, all these SE-genes were used to construct a prognostic signature. The Univariate COX analysis results of 19 significant SE-genes are listed in Table ??.

Next, LASSO regression was performed on the 19 significant SE-genes from univariate COX analysis to screen for candidate genes. The detailed process of LASSO regression and related figures are shown in Fig. ??A,B. Using  $\lambda_{min} = 0.014$ , 18 SE-genes were selected, while 10 SE-genes were selected with  $\lambda_{1se} = 0.055$ . So, we further studied the 18-gene model.

Subsequently, a multivariate Cox regression analysis using stepwise regression was utilized to identify which candidate genes were independently associated with overall survival (OS). Ten genes were excluded due to potential collinearity. Multivariate Cox regression analysis identified *TP53I3*, *ADCY7*, *NQO2*, *CCDC102A*, *ADM*, *SYTL3*, *PSCA* and *BAIAP2* as being independently associated with OS, while *NPR1* had no significant impact on OS (Table ??). Using an optimal cut-off value of 3.06, 265 patients with cervical cancer were divided into a high-risk and a low-risk group. Kaplan-Meier survival analysis showed that the survival of patients could be stratified into different risk groups using the 9-gene model ( $p < 0.05$ ) (Fig. ??A). In addition, as shown in Fig. ??B, the prognosis scores of the different risk groups were significantly different ( $p < 0.001$ ). The performance of the model was assessed using the time-dependent receiver operating characteristic (ROC) curves, which showed a value of 0.82, 0.86 and 0.87 for 1-, 2- and 3-year OS, respectively (Fig. ??C).

Considering the potential impact of clinical factors such as age, clinical stage, survival with tumor and pathological type, we validated the independence of the multi-SE-genes prognostic model using univariate and multivariate Cox regression analyses. In the univariate Cox regression analysis, the risk score of CC patients was related to OS (HR = 7.751, 95% CI = 4.308–13.946,  $p < 0.001$ ) (Fig. ??C). Other important univariate prognostic factors included survival with tumor and clinical stage, both of which demonstrated adverse effects on survival. Subsequently, we used these three prognostic variables to construct a multivariate COX prognostic model. Multivariate COX analysis combined risk score showed that CC patients with higher clinical stage, survival with tumor and the high-risk group had a poorer survival ( $p < 0.05$ ) (Fig. ??D).

Further, the expression levels of *ADCY7*, *CCDC102A*, *ADM* and *SYTL3* were significantly different between the high-risk and low-risk groups ( $P < 0.05$ ), while the expression levels of *BAIAP2*, *NPR1*, *NQO2*, *PSCA* and *TP43I3* were similar between the two groups (Fig. ??). Among the genes with significant differential expression, *ADCY7* and *CCDC102A* showed high expression in the high-risk group and were important poor prognostic factors. K-M survival analysis showed that except for *NPR1*, the expression status of the other 8 SE-genes significantly impacted the prognosis of cervical cancer patients (Fig. ??).

## 4. Discussion

Many studies have reported the involvement of SEs in the growth of malignant tumors and found that they are one of the most important regulatory factors [? ?]. However, these mechanisms remain to be explored [?]. Although targeting the regulation of SEs might be considered a potential therapeutic strategy for cancer treatment, selecting appropriate anti-cancer drugs remains challenging [?]. More and more studies have shown that JQ1 can play an anti-tumor role by interfering with the transcriptional level of the SEs [?]. In this present study, we first verified that JQ1 had a significant inhibitory effect on CC HeLa cells through CCK-8 cell proliferation assay, which was concordant with the results of previous studies in other tumors [? ? ? ?]. Subsequently, we used full

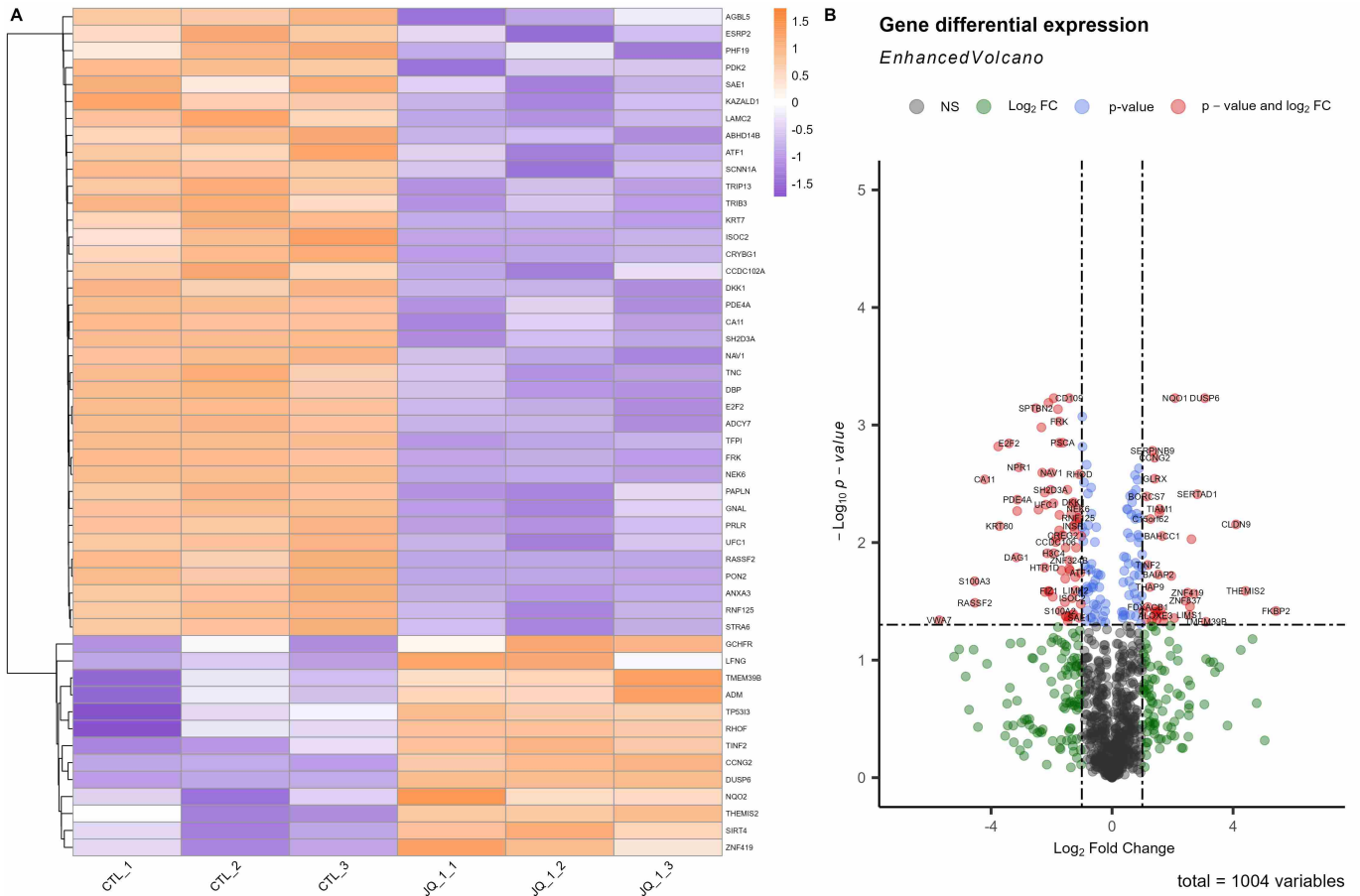


FIGURE 4. Screening and differential expression analysis of SE-genes, illustrated by (A) Heatmap, (B) Volcano map.

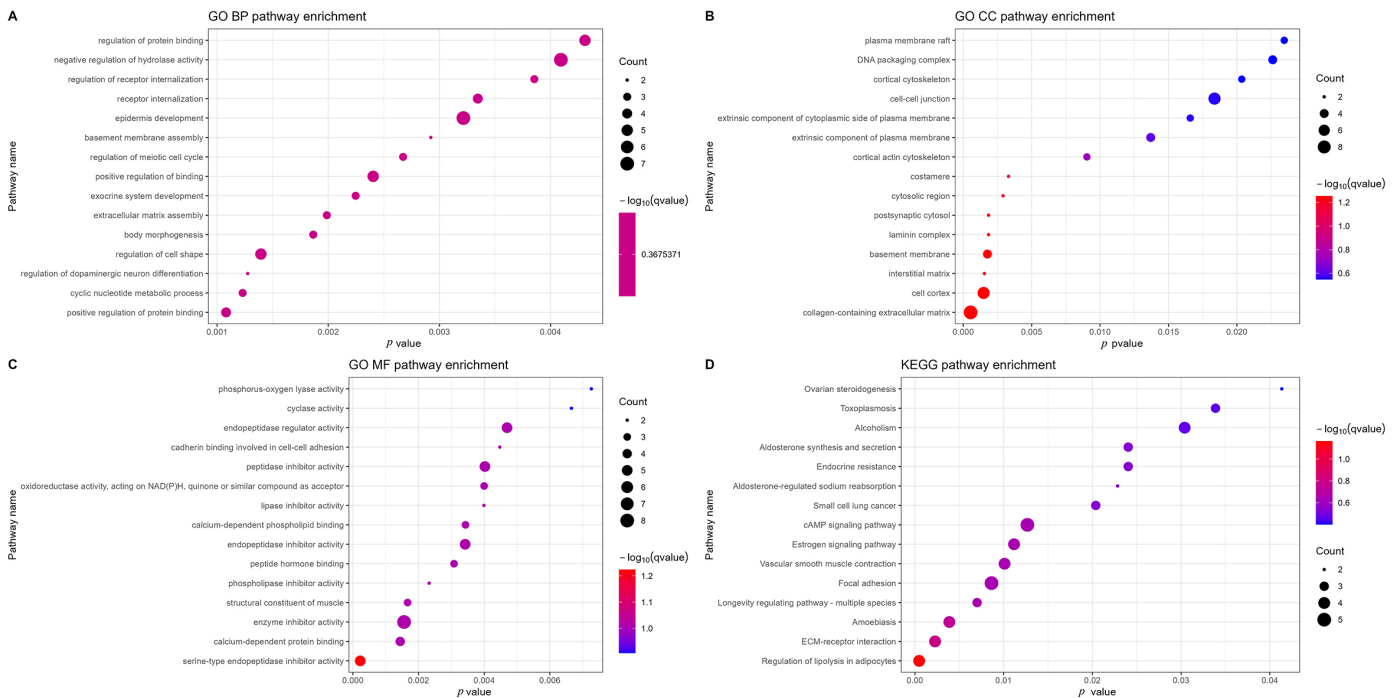


FIGURE 5. Functional annotation and pathway enrichment analysis (FAPEA) of differentially expressed SE-genes. (A) GO biological process enrichment, (B) GO cellular component enrichment, (C) GO molecular function enrichment, (D) KEGG pathway enrichment. GO: Gene Ontology; BP: biological process; CC: cellular component; MF: molecular function; KEGG: Kyoto Encyclopedia of Genes and Genomes.



**TABLE 2. Univariate COX analysis results of significant SE-genes.**

SE-genes	HR	HR.95L	HR.95H	<i>p</i> value
<i>PDK2</i>	0.558	0.330	0.943	0.029
<i>ISOC2</i>	0.551	0.326	0.931	0.026
<i>RASSF2</i>	0.565	0.329	0.970	0.038
<i>PON2</i>	1.798	1.064	3.039	0.028
<i>KAZALD1</i>	0.580	0.339	0.991	0.046
<i>ABHD14B</i>	0.437	0.255	0.751	0.003
<i>TP53I3</i>	2.389	1.399	4.078	0.001
<i>ADCY7</i>	2.042	1.182	3.530	0.011
<i>NQO2</i>	0.400	0.235	0.680	0.001
<i>CCDC102A</i>	1.922	1.140	3.240	0.014
<i>ADM</i>	2.153	1.235	3.754	0.007
<i>SYTL3</i>	0.452	0.265	0.772	0.004
<i>PSCA</i>	0.488	0.286	0.833	0.009
<i>NPR1</i>	0.585	0.346	0.989	0.045
<i>LIMS1</i>	1.724	1.024	2.903	0.041
<i>RHOD</i>	1.998	1.164	3.428	0.012
<i>BAIAP2</i>	0.576	0.342	0.971	0.038
<i>NQO1</i>	0.589	0.349	0.994	0.048
<i>ANXA2</i>	2.063	1.223	3.480	0.007

Note: HR.95L: lower limit of 95% confidence interval; HR.95H: upper limit of 95% confidence interval.

**TABLE 3. Multivariate COX analysis results of 9 SE-genes.**

SE-genes	b	se	HR	HR.95L	HR.95H	<i>p</i> value
<i>TP53I3</i>	1.533	0.328	4.632	2.437	8.803	<0.001
<i>ADCY7</i>	0.826	0.318	2.284	1.225	4.260	0.009
<i>NQO2</i>	-0.836	0.296	0.434	0.243	0.774	0.005
<i>CCDC102A</i>	0.607	0.303	1.835	1.014	3.323	0.045
<i>ADM</i>	1.086	0.331	2.963	1.548	5.673	0.001
<i>SYTL3</i>	-1.359	0.297	0.257	0.144	0.460	<0.001
<i>PSCA</i>	-0.738	0.322	0.478	0.254	0.899	0.022
<i>NPR1</i>	-0.474	0.283	0.622	0.357	1.084	0.094
<i>BAIAP2</i>	-1.152	0.308	0.316	0.173	0.577	<0.001

Note: b: regression coefficient; se: standard error of regression coefficient; HR.95L: lower limit of 95% confidence interval; HR.95H: upper limit of 95% confidence interval.

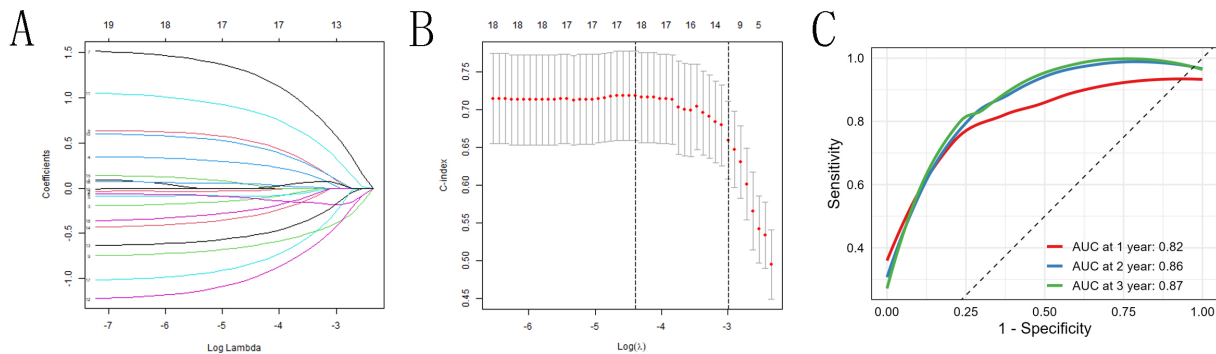


**FIGURE 8. LASSO penalized Cox regression analysis results with (A) regression coefficient plot, (B) regression parameters plot, and (C) time-dependent ROC curve plot. LASSO: least absolute shrinkage and selection operator.**



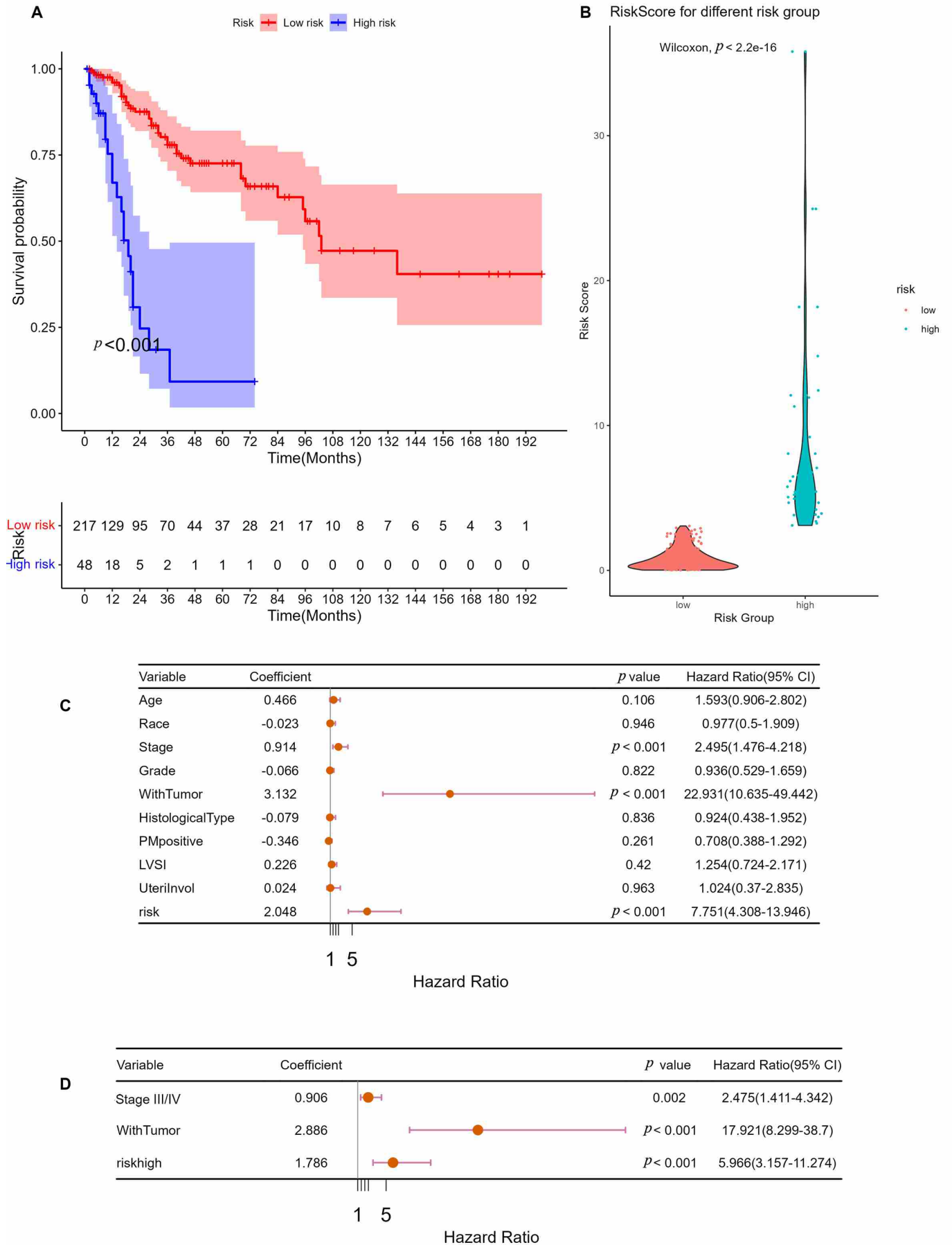


**FIGURE 9. Prognostic value of Riskscore from the prognostic model via SE-genes with (A) Kaplan-Meier Survival Curve, (B) Univariate COX analysis combined with clinical data, (C) Multivariate COX analysis combined with clinical stage. PMpositive: Parametrial invasion positive; LVS1: lymph-vascular space invasion; UteriInvol: Uterine invasion.**

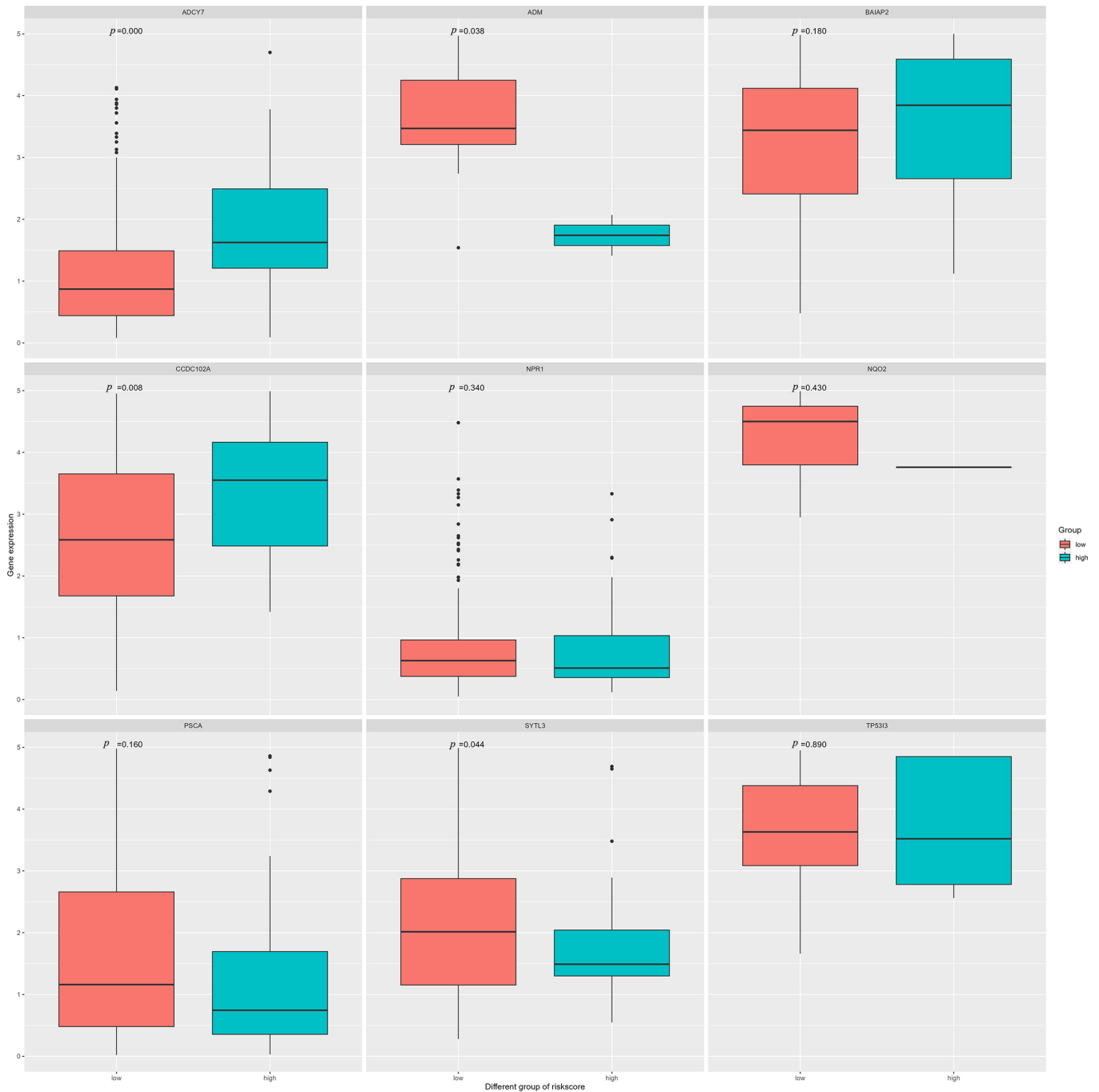


**FIGURE 10. Differential expression analysis of important SE-genes included in the prognostic model.**

transcriptome sequencing to explore the gene expression level of HeLa cells with or without JQ1 treatment. As expected, we found that JQ1 changed the gene expression profile of HeLa cells, and some of these genes were identified as SE-related genes. Currently, the dbCoRC and Cistrome DB databases are mainly used to identify SE-related genes. Although some genes were found to play a prognostic role in other malignant tumors, the functions of most of these genes are yet to be clarified [?]. In this present study, we identified 110 SE-genes that were differentially expressed between HeLa cells treated with or without JQ1, of which 72 were downregulated and 38 were upregulated. Investigations at the transcriptional level showed that JQ1 might exhibit anti-tumor functions through SE-related genes.

Next, we performed functional annotation and pathway enrichment analysis on the identified DEGs. KEGG pathway enrichment analysis revealed that candidate genes were mainly enriched in the regulation of lipolysis in adipocytes, ECM-receptor interaction, amoebiasis, longevity regulating pathway—multiple species, focal adhesion and other pathways. These pathways were related to immune response, amino acid metabolism, cell proliferation, protein transport and other physiological and biochemical reactions. Hub genes, including *LAMC2*, *LAMB3*, *DAG1*, *TIAM1*, *BAIAP2*, *RHOD*, *ADCY7*, *GNAL* and *PDE4A*, were identified through PPI network analysis and MCODE analysis. Two hub genes, namely *ADCY7* and *BAIAP2*, were included in our proposed 9-gene prognostic model, in which high expression of *ADCY7*

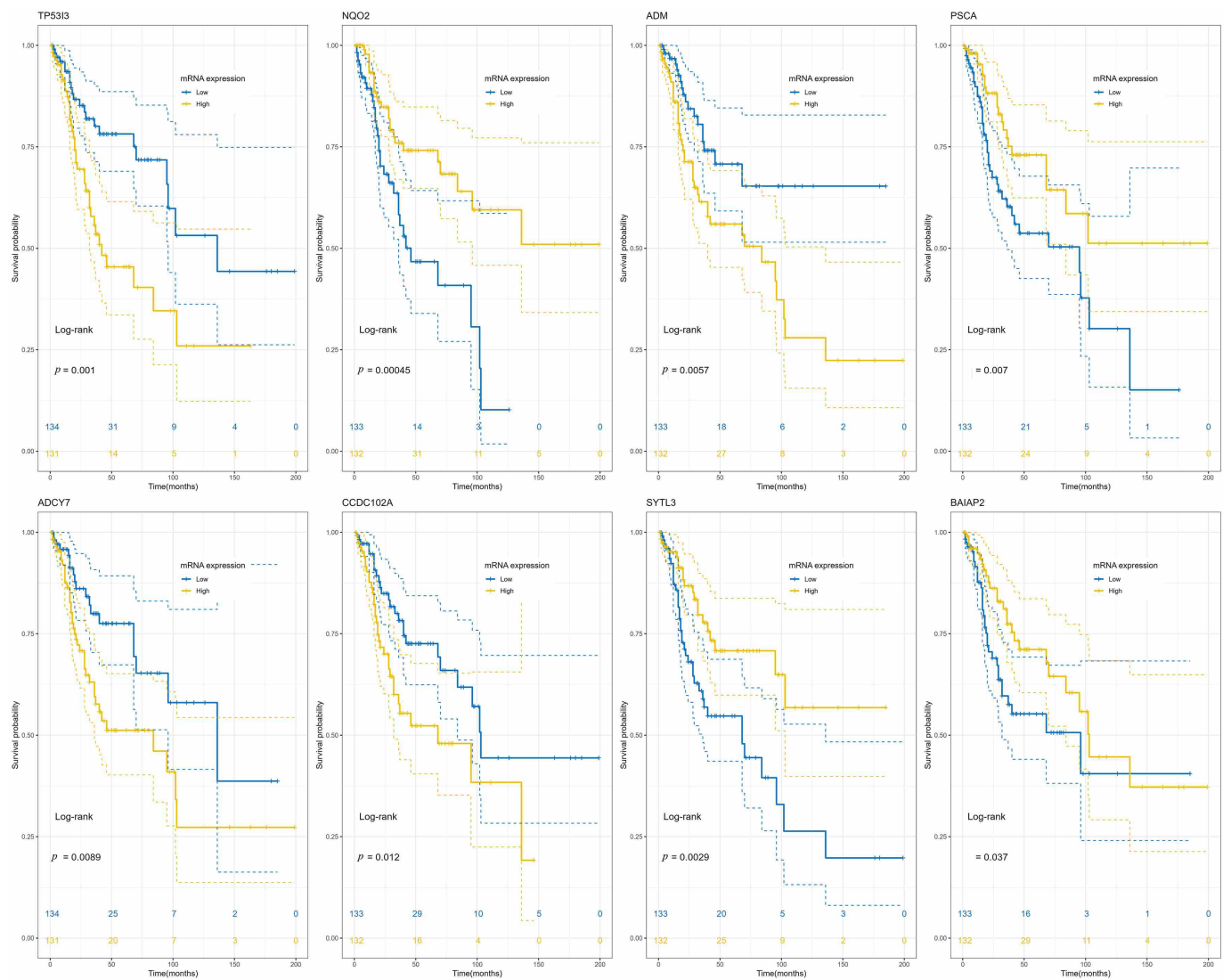


**FIGURE 11. Survival curves of SE-genes of interest.**

was associated with poor prognosis and high expression of *BAIAP2* was associated with better prognosis.

Lastly, we proposed a risk-score formula by constructing a signature using the 9 SE-associated genes specific for CC. We found that of the 9 genes included in the model, only one gene (*NPR1*) was not independently associated with survival, while the other 8 genes had excellent performance in the prognosis model, which also demonstrated important predictive values in separate K-M survival analysis. The performance of the model was determined *via* time-dependent ROC curves, which showed that the 1-, 2- and 3-year OS was associated with a value of 0.82, 0.86 and 0.87, respectively, suggesting that the model had feasible and creditable prognostic prediction abilities.

Previous studies reported that JQ1 had a significant inhibitory effect on the proliferation of cancer cells, and this inhibitory effect was time- and concentration-dependent [? ?]. In our exploratory experiment, we also found that the inhibition of JQ1 on HeLa cells was time- and concentration-dependent. Existing literature showed that JQ1 significantly inhibited various malignant tumor cells of different genetic backgrounds [? ?]. To the best of our current knowledge,

only few studies have explored the anti-cancer mechanism of JQ1 in CC [? ?]. To understand the anti-tumor mechanism of JQ1 in cervical cancer, we designed the present experiment to explain the potential mechanism at the gene expression level.

SEs represent a large cluster of active enhancers essential to maintain cell identity and drive the expression of some oncogenes in different cancers [?]. The activation of SEs suggests that the functions of some of these oncogenes could be strongly regulated, including lncRNAs, miRNAs and mRNAs. The differential expression of mRNAs ultimately determines the biological characteristics of cancer cells, such as stronger proliferation or inhibition of apoptosis [?], which can be considered as the functional executors of SE [?]. Consequently, our research focused on SE-related genes that belong to mRNAs. By matching SE, we obtained 110 SE-genes differentially expressed in the Cistrome DB database. In this current study, LASSO penalized Cox regression and univariate and multivariate Cox regression analyses were utilized to narrow the range of the candidate genes. Then, we successfully established a 9-gene risk score model for survival prediction, comprising *TP5313*, *ADCY7*, *NQO2*, *CCDC102A*, *ADM*, *SYTL3*, *PSCA*, *BAIAP2* and *NPR1*. We found that

*ADCY7* and *CCDC102A* were highly expressed in the high-risk group, indicating that the two genes were associated with poor prognosis of CC patients. On the other hand, *ADM* and *SYTL3* genes showed low expression in the high-risk group, where the high expression of *SYTL3* was beneficial to the prognosis of CC patients.

Our research also focused on the inhibitory effects of JQ1 on CC HeLa cells and obtained the differential gene expression profile of JQ1 through transcriptional sequencing, based on which we identified SE-related genes and constructed a 9-gene prognosis model. Our research showed that altered SE-related genes play an important prognostic role in cervical cancer patients, which has important clinical significance in predicting the prognosis of CC patients. However, despite the clinical significance of our results, there were some limitations associated with our research. First, the development and progression of cancer are regulated by a series of gene sets, and the mechanism is complex and extensive, while in this study, we only focused on SE-related regulation, as we believe it is crucial in CC. Second, due to the limitations of direct exploration of SEs in research, it might be more convenient to explore the biological functions of SEs by taking the target genes of SEs as the entry point. However, this means that the relevant mechanism interpretation would be indirect, requiring further verification and discussion. Lastly, although some SE-genes were found to be associated with the prognosis of CC, their exact biological role in CC remains unclear. The functions of these genes should be further investigated in *in vitro* and *in vivo* settings.

## 5. Conclusions

In conclusion, our findings indicated that JQ1 significantly suppressed the proliferation of CC HeLa cells. JQ1 likely exerts its anti-tumor effects by modifying the transcriptional activity of SEs and influencing the expression of SE-related genes. By analyzing differently expressed SE-genes induced by JQ1, we constructed a 9-gene prognostic model that showed promising abilities to independently predict the survival of CC patients. Additionally, *TP53I3*, *ADCY7*, *NQO2*, *CCDC102A*, *ADM*, *SYTL3*, *PSCA*, *BAIAP2* and *NPR1* were identified as potential SE-associated genes in CC and may play crucial roles in the development and progression of this cancer.

## AVAILABILITY OF DATA AND MATERIALS

Publicly available datasets were analyzed in this study. This data can be found here: The Cancer Genome Atlas Program (TCGA, <https://www.cancer.gov/about-nci/organization/ccg/research/structural-genomics/tcga>). Further inquiries can be directed to the corresponding authors.

## AUTHOR CONTRIBUTIONS

JQZ and FJH—Conception and design; YXL and BFH—Provision of study materials or patients; JQZ, FJH and BFH—Collection and assembly of data; JQZ and BFH—Data analysis and interpretation; YXL, BFH, FJH and JQZ—Manuscript

writing and editing. All authors contributed to the article and approved the submitted version.

## ETHICS APPROVAL AND CONSENT TO PARTICIPATE

Not applicable.

## ACKNOWLEDGMENT

Not applicable.

## FUNDING

This study was supported in part by the China Postdoctoral Science Foundation (Grant No: 2021M700779 to He F), the Medical Research Fund of Guangdong Province (Grant No: A2022044 to He F), Fujian provincial health technology project (Youth Scientific Research Project, 2019-1-50 to Zheng J) and the Nursery Fund Project of the Second Affiliated Hospital of Fujian Medical University (Grant No: 2021MP05 to Zheng J).

## CONFLICT OF INTEREST

The authors declare that the research was conducted without any commercial or financial relationships that could be construed as a potential conflict of interest.

## SUPPLEMENTARY MATERIAL

Supplementary material associated with this article can be found, in the online version, at <https://oss.ejgo.net/files/article/1713758016784744448/attachment/Supplementary%20material.zip>.

## REFERENCES

- [1] Siegel R L, Miller K D, Fuchs H E, Jemal A. Cancer Statistics, 2021. CA: A Cancer Journal for Clinicians. 2021; 71: 7–33.
- [2] Chen W, Zheng R, Baade PD, Zhang S, Zeng H, Bray F, *et al.* Cancer statistics in China, 2015. CA: A Cancer Journal for Clinicians. 2016; 66: 115–132.
- [3] Yoneda JY, Teixeira JC, Derchain S, Bragança JF, Zeferino LC, Vale DB. Screen-and-treat approach in managing cervical cancer precursor lesions: an observational study with 524 women. European Journal of Obstetrics & Gynecology and Reproductive Biology. 2023; 280: 78–82.
- [4] Xie Y, Kong W, Zhao X, Zhang H, Luo D, Chen S. Immune checkpoint inhibitors in cervical cancer: current status and research progress. Frontiers in Oncology. 2022; 12: 984896.
- [5] Xu Q, Wang J, Sun Y, Lin Y, Liu J, Zhuo Y, *et al.* Efficacy and safety of sintilimab plus anlotinib for PD-L1—positive recurrent or metastatic cervical cancer: a multicenter, single-arm, prospective phase II trial. Journal of Clinical Oncology. 2022; 40: 1795–1805.
- [6] Zhang L, Mao Z, Lai Y, Wan T, Zhang K, Zhou B. A review of the research progress in T-lymphocyte immunity and cervical cancer. Translational Cancer Research. 2020; 9: 2026–2036.
- [7] Parker S C, Stitzel M L, Taylor D L, Orozco JM, Erdos MR, Akiyama JA, *et al.* Chromatin stretch enhancer states drive cell-specific gene regulation and harbor human disease risk variants. Proceedings of the National

- Academy of Sciences of the United States of America. 2013; 110: 17921–17926.
- [8] Whyte W, Orlando D, Hnisz D, Abraham B, Lin C, Kagey M, *et al.* Master transcription factors and mediator establish super-enhancers at key cell identity genes. *Cell*. 2013; 153: 307–319.
- [9] Lovén J, Hoke H, Lin C, Lau A, Orlando D, Vakoc C, *et al.* Selective inhibition of tumor oncogenes by disruption of super-enhancers. *Cell*. 2013; 153: 320–334.
- [10] Qi T, Qu J, Tu C, Lu Q, Li G, Wang J, *et al.* Super-enhancer associated five-gene risk score model predicts overall survival in multiple myeloma patients. *Frontiers in Cell and Developmental Biology*. 2020; 8: 596777.
- [11] Jiang Y, Lin D, Mayakonda A, Hazawa M, Ding L, Chien W, *et al.* Targeting super-enhancer-associated oncogenes in oesophageal squamous cell carcinoma. *Gut*. 2017; 66: 1358–1368.
- [12] Liang X, Meng Y, Li C, Liu L, Wang Y, Pu L, *et al.* Super-enhancer-associated nine-gene prognostic score model for prediction of survival in chronic lymphocytic leukemia patients. *Frontiers in Genetics*. 2022; 13: 1001364.
- [13] Wadhwa E, Nicolaidis T. Bromodomain inhibitor review: bromodomain and extra-terminal family protein inhibitors as a potential new therapy in central nervous system tumors. *Cureus*. 2016; 8: e620.
- [14] Li X, Duan Y, Hao Y. Identification of super enhancer-associated key genes for prognosis of germinal center B-cell type diffuse large B-cell lymphoma by integrated analysis. *BMC Medical Genomics*. 2021; 14: 69.
- [15] Barbieri I, Cannizzaro E, Dawson MA. Bromodomains as therapeutic targets in cancer. *Briefings in Functional Genomics*. 2013; 12: 219–230.
- [16] Noguchi-Yachide T. BET bromodomain as a target of epigenetic therapy. *Chemical and Pharmaceutical Bulletin*. 2016; 64: 540–547.
- [17] Wang L, Xu M, Kao C, Tsai SY, Tsai M. Small molecule JQ1 promotes prostate cancer invasion *via* BET-independent inactivation of FOXA1. *Journal of Clinical Investigation*. 2020; 130: 1782–1792.
- [18] Baldan F, Allegri L, Lazarevic M, Catia M, Milosevic M, Damante G, *et al.* Biological and molecular effects of bromodomain and extra-terminal (BET) inhibitors JQ1, IBET-151, and IBET-762 in OSCC cells. *Journal of Oral Pathology & Medicine*. 2019; 48: 214–221.
- [19] Han D, Qu L, Sun L, Sun Y. Variable selection for a mark-specific additive hazards model using the adaptive LASSO. *Statistical Methods in Medical Research*. 2021; 30: 2017–2031.
- [20] Huang M, Chen Y, Yang M, Guo A, Xu Y, Xu L, *et al.* DbCoRC: a database of core transcriptional regulatory circuitries modeled by H3K27ac ChIP-seq signals. *Nucleic Acids Research*. 2018; 46: D71–D77.
- [21] Mei S, Qin Q, Wu Q, Sun H, Zheng R, Zang C, *et al.* Cistrome data browser: a data portal for ChIP-Seq and chromatin accessibility data in human and mouse. *Nucleic Acids Research*. 2017; 45: D658–D662.
- [22] Thandapani P. Super-enhancers in cancer. *Pharmacology & Therapeutics*. 2019; 199: 129–138.
- [23] Li G, Qu Q, Qi T, Teng X, Zhu H, Wang J, *et al.* Super-enhancers: a new frontier for epigenetic modifiers in cancer chemoresistance. *Journal of Experimental & Clinical Cancer Research*. 2021; 40: 174.
- [24] Sengupta S, George RE. Super-enhancer-driven transcriptional dependencies in cancer. *Trends in Cancer*. 2017; 3: 269–281.
- [25] He Y, Long W, Liu Q. Targeting super-enhancers as a therapeutic strategy for cancer treatment. *Frontiers in Pharmacology*. 2019; 10: 361.
- [26] Liu B, Liu X, Han L, Chen X, Wu X, Wu J, *et al.* BRD4-directed super-enhancer organization of transcription repression programs links to chemotherapeutic efficacy in breast cancer. *Proceedings of the National Academy of Sciences*. 2022; 119: e2109133119.
- [27] Alghamdi S, Khan I, Beeravolu N, McKee C, Thibodeau B, Wilson G, *et al.* BET protein inhibitor JQ1 inhibits growth and modulates WNT signaling in mesenchymal stem cells. *Stem Cell Research & Therapy*. 2016; 7: 22.
- [28] Bagratuni T, Mavrianou N, Gavalas NG, Tzannis K, Arapinis C, Lontos M, *et al.* JQ1 inhibits tumour growth in combination with cisplatin and suppresses JAK/STAT signalling pathway in ovarian cancer. *European Journal of Cancer*. 2020; 126: 125–135.
- [29] CHOI SK, HONG SH, KIM HS, SHIN CY, NAM SW, CHOI WS, *et al.* JQ1, an inhibitor of the epigenetic reader BRD4, suppresses the bidirectional MYC-AP4 axis *via* multiple mechanisms. *Oncology Reports*. 2016; 35: 1186–1194.
- [30] Wang J, Ma X, Ma J. Identification of four enhancer-associated genes as risk signature for diffuse glioma patients. *Journal of Molecular Neuroscience*. 2022; 72: 410–419.
- [31] Zanellato I, Colangelo D, Osella D. JQ1, a BET inhibitor, synergizes with cisplatin and induces apoptosis in highly chemoresistant malignant pleural mesothelioma cells. *Current Cancer Drug Targets*. 2018; 18: 816–828.
- [32] Wang L, Wu X, Huang P, Lv Z, Qi Y, Wei X, *et al.* JQ1, a small molecule inhibitor of BRD4, suppresses cell growth and invasion in oral squamous cell carcinoma. *Oncology Reports*. 2016; 36: 1989–1996.
- [33] Zhang Y, Duan S, Jang A, Mao L, Liu X, Huang G. JQ1, a selective inhibitor of BRD4, suppresses retinoblastoma cell growth by inducing cell cycle arrest and apoptosis. *Experimental Eye Research*. 2021; 202: 108304.
- [34] Zhang Z, Zhang Q, Xie J, Zhong Z, Deng C. Enzyme-responsive micellar JQ1 induces enhanced BET protein inhibition and immunotherapy of malignant tumors. *Biomaterials Science*. 2021; 9: 6915–6926.
- [35] Wang Y, Shen N, Li S, Yu H, Wang Y, Liu Z, *et al.* Synergistic therapy for cervical cancer by codelivery of cisplatin and JQ1 inhibiting Plk1-mutant Trp53 axis. *Nano Letters*. 2021; 21: 2412–2421.
- [36] Rataj O, Haedicke-Jarboui J, Stubenrauch F, Iftner T. Brd4 inhibition suppresses HPV16 E6 expression and enhances chemoresponse: a potential new target in cervical cancer therapy. *International Journal of Cancer*. 2019; 144: 2330–2338.
- [37] Kai Y, Li B E, Zhu M, Li GY, Chen F, Han Y, *et al.* Mapping the evolving landscape of super-enhancers during cell differentiation. *Genome Biology*. 2021; 22: 269.

**How to cite this article:** Yuxi Lin, Bifen Huang, Fangjie He, Jianqing Zheng. *BRD4* inhibitor JQ1 may affect the prognosis of cervical cancer through super-enhancer-related genes. *European Journal of Gynaecological Oncology*. 2023; 44(5): 26-38. doi: 10.22514/ejgo.2023.076.